STIM1-induced precortical and cortical subdomains of the endoplasmic reticulum

Lelio Orci[1], Mariella Ravazzola, Marion Le Coadic, Wei-wei Shen, Nicolas Demaurex, and Pierre Cosson[1]

Department of Cell Physiology and Metabolism, University of Geneva Medical School, 1211 Geneva 4, Switzerland

Contributed by Lelio Orci, October 2, 2009 (sent for review July 15, 2009)

Store-operated calcium entry relies on the formation of a specialized compartment derived from the endoplasmic reticulum (ER) and closely apposed to the plasma membrane. In this study, detailed ultrastructural analysis revealed the existence of three distinct structures derived from conventional ER: precortical ER, cortical ER, and thin cortical ER. Precortical subdomains of the ER enriched in STIM1 can form without contacting the plasma membrane. Upon ER calcium depletion, these subdomains are translocated to the plasma membrane to form cortical ER, which is still connected to the conventional ER. Thin cortical ER, depleted of BiP and deprived of attached ribosomes, may represent a specialized region dedicated to calcium regulation and not engaged in protein translocation and folding. These observations form the basis for future structure-function analysis of cortical ER.

calcium | store-operated calcium entry

The endoplasmic reticulum (ER) plays a key role in calcium homeostasis in eukaryotic cells (1). It represents the major intracellular store of calcium and controls calcium influx through the plasma membrane (PM), a process referred to as store-operated calcium entry (SOCE). SOCE is orchestrated by the ER membrane protein STIM1, which, upon calcium depletion, accumulates into ER domains located beneath the PM and activates the Orai family of calcium channels (reviewed in ref. 2).

The mechanism by which STIM1 is concentrated in regions of the ER apposed to the PM has been a subject of intense investigations in recent years. Upon depletion of calcium in the ER, the luminal domain of STIM1 forms multimers (3), and STIM1 is detected by immunofluorescence in punctae underneath the PM (4, 5). The interaction of STIM1 with surface Orai1 causes opening of the Orai1 channels and calcium entry in the cell (6). The cytosolic domain of STIM1 is essential for its relocation to peripheral ER and it is believed to act through at least two distinct synergistic mechanisms. First, interaction between the cytosolic domains of STIM1 and Orai1 is sufficient to target STIM1 to peripheral ER (7, 8). Second, it has been postulated that STIM1 can be targeted to peripheral ER by an Orai1-independent mechanism, which requires its lysine-rich C-terminal portion. This possibility would notably account for the observation that when STIM1 is expressed in the absence of Orai1, it can still be targeted to peripheral ER (9) and that this targeting requires its C terminus (8).

Surprisingly, little ultrastructural analysis of STIM1-induced peripheral ER has been performed. In the best study published to date (10), calcium depletion induced a modest increase (+50%) of ER present within 50 nm of the PM, visualized with an ER-specific HRP-KDEL fusion protein. HRP-STIM1 was observed in conventional ER cisternae, as well as in "tubules" located within 50 nm of the PM. Upon calcium depletion, HRP-STIM1 was depleted from cytosolic cisternae, and the number and length of HRP-positive tubules close to the PM increased.

In another study, a series of elegant experiments was designed to analyze interactions between the PM and ER, making use of a chemically inducible bridge formation between the PM and the ER membrane (11). Upon thapsigargin (Tg) treatment, YFP-STIM1 formed clusters only at the periphery of zones of tight apposition (4–6 nm), suggesting that its contact with the PM involved a large molecular complex with an estimated 10- to 14-nm protrusion in the cytoplasm. This interpretation was in good agreement with ultrastructural evidence indicating that the minimal distance between peripheral ER and PM ranged from 10 to 25 nm (average 17 nm) (10). This large ER–PM gap had important functional implications, as it suggested that a large putative protein complex may mediate the interaction between Orai1 and STIM1. However, more recent evidence indicates a direct contact between Orai1 and STIM1 (8).

The main goal of the present study was to provide a detailed ultrastructural description of the ER remodeling induced by STIM1, to gain new insights into the mechanisms driving its formation. Our results distinguish at least three elements in the formation of cortical ER: precortical structures formed in the cytosol, cortical ER apposed to the PM, and thin cortical ER devoid of ribosomes.

Results

Cortical ER Is a Heterogeneous Subdomain of the ER. To analyze the formation of cortical ER, we used HeLa cells transfected with a plasmid-expressing YFP-tagged STIM1. We first analyzed by electron microscopy the structure of peripheral ER in cells fixed and embedded in Epon in situ. This procedure preserves optimally cellular architecture and maintains the orientation of the cells relative to the substrate. Before fixation, cells were either left untreated, or exposed to 1-μM Tg for 10 min to deplete calcium in the ER and elicit SOCE. In treated cells, we observed segments of the ER closely apposed to the PM (Fig. 1 *A*–*C*), with an average length of 200 to 400 nm, and often aligned along microtubules (sectioned transversally in Fig. 1*B*, longitudinally in Fig. 1*C*). Because of their presence in the cortex of the cells, we refer to these structures as "cortical ER" (cER) in this study. Although cER often appeared as tubules in individual sections, serial sectioning revealed that it corresponds virtually always to large flattened sheets of ER closely apposed to the PM and still connected to conventional ER cisternae [see Fig. 1*A* and supporting information (SI) Fig. S1]. The average distance between the PM and cER was 8.3 ± 0.3 nm (mean + SEM; n = 105 measures, 30 pictures). Huge variations were observed however, with individual distances ranging from 1.3 nm to 14.7 nm. In Fig. 1*A*, an arrow points to a region of very close contact between the ER and the PM. A similar distance between cER and the PM was observed in cryosections (11.3 ± 2.9 nm; n = 108; minimum 3.8 nm, maximum 16.9 nm). Ribosomes were absent from the face of cER cisternae facing the PM, but frequently seen attached to the opposite face (see Fig. 1*B*). Although cER was observed in both stimulated and nonstimulated cells, the amount of cER increased significantly upon calcium depletion (approximately fourfold) (Table 1).

Close scrutiny revealed that approximately half of the cER exhibited a distinct morphology (see Fig. 1), referred to here as "thin cER." Thin cER cisternae presented all of the features of cER described above, but in addition they were thinner [thickness: 24 ± 0.4 nm (n = 111) versus 73 ± 3 nm (n = 85) for conventional ER cisternae] and deprived of attached

Author contributions: L.O., M.R., M.L.C., W.-w.S., N.D., and P.C. designed research, performed research, analyzed data, and wrote the paper.

The authors declare no conflict of interest.

Freely available online through the PNAS open access option.

[1]To whom correspondence may be addressed. pierre.cosson@unige.ch or lelio.orci@unige.ch.

This article contains supporting information online at www.pnas.org/cgi/content/full/0911280106/DCSupplemental.

www.pnas.org/cgi/doi/10.1073/pnas.0911280106

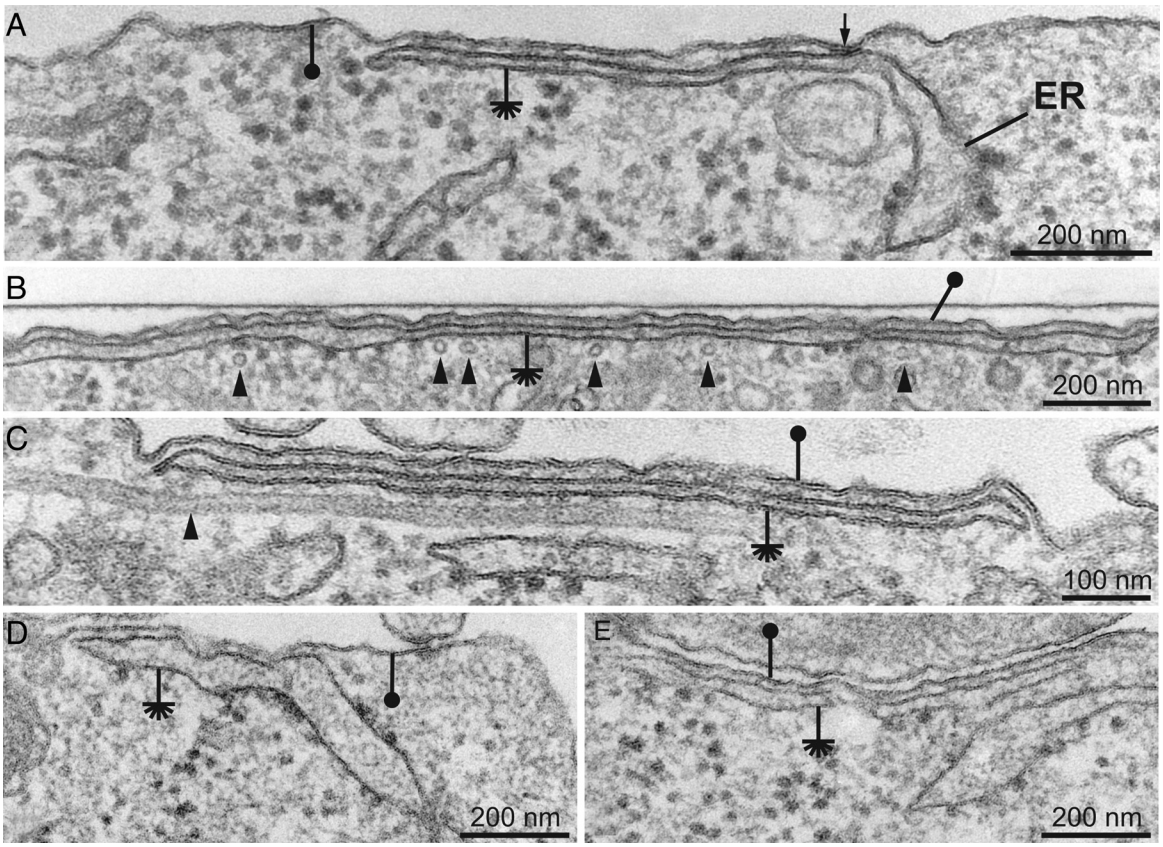

Fig. 1. Calcium depletion stimulates the formation of cortical ER. HeLa cells were treated for 10 min with Tg (1 μM) to deplete ER calcium stores. They were then fixed, embedded in Epon resin, sectioned and observed. (*A–C*) In cells transfected with YFP-STIM1, calcium depletion induced the formation of large sheets of cER (asterisks) apposed to the PM (closed circle), which were often aligned along microtubules (arrowheads). Note the connection between cER and ER cisternae (ER) in *A*, as well as a region of very close contact between the PM and the cER (arrow). Ribosomes were seen only on thick regions of cER, but absent in thinner regions. The bottom of the culture dish appears in (*B*) as a straight, dense line on top of the picture. (*D* and *E*) In nontransfected HeLa cells, local apposition of the ER to the PM also became apparent upon Tg treatment. Both thick (*D*) and thin (*E*) cER was observed. The corresponding quantitative analysis is presented in Table 1.

ribosomes, even on the side facing the cytosol (see Fig. 1*A* and *C*). This thinness was particularly evident in certain pictures, where thin ribosome-free regions alternated with slightly thicker regions harboring ribosomes (see Fig. 1*B*).

Intriguingly, cER was much more abundant on the basal membrane (facing the substrate) than on the apical membrane (facing the medium) (see Table 1), revealing that although HeLa cells are poorly polarized, the apical membrane presents specific features that limit the formation of cER. In lateral domains (defined here as regions of the cell directly facing another cell, but not necessarily engaged into close contact), more variability was observed, but overall the amount of cER was similar to that seen on basal membranes (see Table 1).

In HeLa cells not transfected with YFP-STIM1, the basal amount of cER was lower than in transfected cells (approximately sixfold) (see Table 1). However, as in transfected cells, the amount of cER increased significantly in nontransfected cells upon calcium depletion (approxi-

Table 1. Quantification of cortical ER in Epon sections

			% of cell surface with cER		
YFP-STIM1	Tg*	Domain	Exp. 1	Exp. 2	Total
No	No (n = 27)	Apical	0.03	0.18	0.11
		Lateral	0.17	0.22	0.19
		Basal	0	0.59	0.37
		Total	0.07	0.37	0.23
No	10 min (n = 39)	Apical	0.73	0.50	0.63
		Lateral	2.05	2.00	2.07
		Basal	0.96	0.94	0.95
		Total	1.17	1.30	1.24
Yes	No (n = 44)	Apical	0.23	0.64	0.36
		Lateral	2.33	0.42	1.81
		Basal	1.95	2.26	2.11
		Total	1.40	1.28	1.40
Yes	10 min (n = 58)	Apical	2.26	3.25	2.66
		Lateral	6.70	4.80	6.28
		Basal	4.92	12.74	8.26
		Total	4.15	7.51	5.44

*The total number of complete cell profiles analyzed is specified for each condition.

Table 2. Labeling density of GFP and BiP on cryosections of HeLa cells transfected with YFP-STIM1

		Mean ± SEM	
	Tg	GFP (Gold/μm)	Bip (Gold/μm^2)
Cortical ER	No	6.9 ± 0.7 n = 30*	40 ± 8 n = 30
	1 min	5.7 ± 0.7 n = 24	32 ± 16 n = 24
	10 min	5.9 ± 0.4 n = 30	29 ± 7 n = 30
Conventional ER	No	1.6 ± 0.3 n = 51	270 ± 15 n = 51
	1 min	1.1 ± 0.2 n = 76	332 ± 29 n = 76
	10 min	0.6 ± 0.1 n = 48†	395 ± 42 n = 48

n, number of structures evaluated.
*In cells not treated with Tg, the intensity of labeling of BiP and GFP are significantly different ($P < 0.01$) in cER and in conventional ER.
†The intensity of STIM1 labeling in conventional ER is significantly lower ($P < 0.01$) in cells treated for 10 min with Tg than in untreated cells.

CELL BIOLOGY

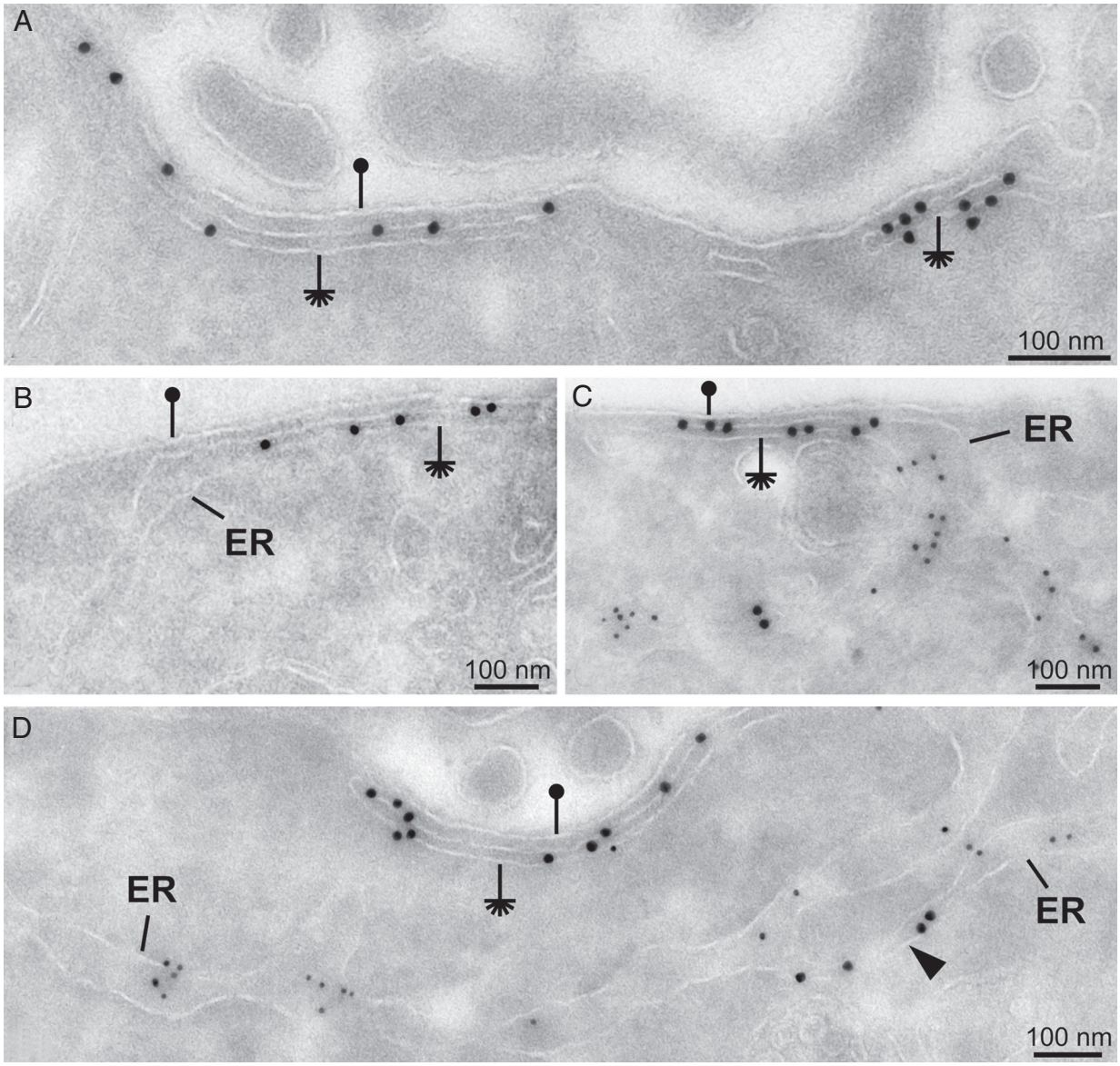

Fig. 2. Thin cER is enriched in STIM1 and depleted of BiP. HeLa cells expressing YFP-STIM1 were fixed and processed for cryo-immuno electron microscopy. (*A* and *B*) YFP-STIM1, revealed with an anti-GFP antibody and 15-nm diameter gold particles was highly enriched in thin cER (asterisks) apposed to the PM (closed circle) relative to conventional ER cisternae (ER). (*C* and *D*) Colabeling with anti-GFP (15-nm diameter gold) and anti-BiP (10-nm diameter gold). BiP is excluded from cER. The corresponding quantitative analysis is presented in Table 2. In an area distant from the PM, a thin ER region enriched in STIM1 and depleted of BiP is visible (arrowhead in *D*).

mately fivefold) (see Table 1), suggesting that similar calcium-sensing mechanisms are at play in transfected and nontransfected cells. Cortical ER profiles were shorter (average 100–200 nm) and less frequent, making their observation more difficult. We did, however, observe cER exhibiting a morphology similar to that seen in transfected cells, as well as several instances of thin cER (see Fig. 1 *D* and *E*). Together, these observations indicate that expression of YFP-STIM1 increased the amount of cER, but did not alter grossly its morphology or its formation in response to calcium depletion.

BiP Is Excluded from Cortical ER. Previously published fluorescence pictures suggested to us that a GFP protein targeted to the ER by a KDEL motif (GFP-KDEL) is excluded from STIM1-enriched punctae (see figure 3 of ref. 4 and figure 4*C* of ref. 5), a result also compatible with our own observations (Fig. S2). However, it is virtually impossible to establish this point with certainty, given the limitations of optical microscopy.

Because BiP is localized in the ER by virtue of its C-terminal KDEL sequence, we performed immunolabeling on cryosections to detect YFP-STIM1 and the luminal chaperone BiP. As expected, YFP-STIM1 was highly enriched in cER relative to conventional ER (Fig. 2 and Table 2). Remarkably, YFP-STIM1 immunoreactivity was concentrated only in thin regions of the cER and not in thicker regions of the ER, even when those were apposed to the PM (see Fig. 2 *B* and *C*). BiP was present at a very low concentration in thin cER, even taking into account the smaller volume of this compartment (see Fig. 2 *C* and *D* and Table 2). Interestingly, in cells not treated with Tg, where cER was less developed, segregation of YFP-STIM1 and depletion of BiP was also observed (see Table 2), suggesting that cER is qualitatively similar in cells with replete calcium stores. Note, however, that most of the YFP-STIM1-enriched cER seen in unstimulated cells corresponds to punctae evoked by the expression of exogenous YFP-STIM1 (see Table 1). High-quality antibodies to STIM1 will be necessary to determine the localization of endogenous STIM1 in nontransfected cells before and after Tg stimulation. Upon calcium depletion, the concentration of YFP-STIM1 in cER did not increase, while it de-

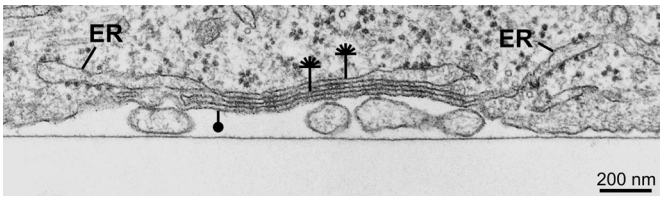

Fig. 3. Formation of double-layered cortical ER. HeLa cells transfected with YFP-STIM1 and depleted of calcium occasionally exhibited two layers of cortical ER (asterisks) apposed to the PM (closed circle). The bottom of the culture dish appears as a straight, dense line below the cell. Analysis of serial sections revealed that the cisterna facing the cytosol did not establish a contact with the PM (Fig. S3).

creased significantly in conventional ER (see Table 2). Together with our observation that the amount of cER increased in these cells upon stimulation (see Table 1), this result demonstrates that in transfected cells, Tg-induced translocation of YFP-STIM1 to the cortical region is primarily caused by an increase in the amount of cER, rather than by a rise in the concentration of YFP-STIM1 in preexisting cER. These observations indicate that, although it is still physically connected to conventional ER, cortical ER represents a subdomain of the ER with a specific composition.

Precortical ER Can Form Without Contacting the PM. Three surprising observations indicated that ER subdomains similar to cER (referred to here as "precortical ER") can form without directly contacting the PM. First, we occasionally observed in Tg-treated cells two superimposed layers of thin cER apposed to the PM (Fig. 3). Serial sectioning revealed that the two cisternae were not connected, and that there was no direct contact between the second layer of cER and the PM (Fig. S3). Second, in cells expressing a constitutively-active mutant of STIM1 (4), cER was abundant even in non-stimulated cells (Fig. S4), and remarkably organized multilayered thin ER structures enriched in STIM1 were seen adjacent to the PM (Fig. 4). Only one cisterna of the stack established a direct contact with the PM. Similar structures were even seen in the cytosol, far from the PM (Fig. S5). Third, in Epon sections we frequently observed regions of ER cisternae distant from the PM that appeared thinner, devoid of ribosomes, and extending along microtubules (Fig. 5 *A* and *B*, *arrows*), and which may represent precortical subdomains. To verify this, we examined cryosections to detect BiP and YFP-STIM1. We indeed observed thinner subdomains of the ER, enriched in STIM1 and depleted of BiP, in areas distant from the PM (see Fig. 2*D*, *arrowheads*, and Fig. 5 *C* and *D*).

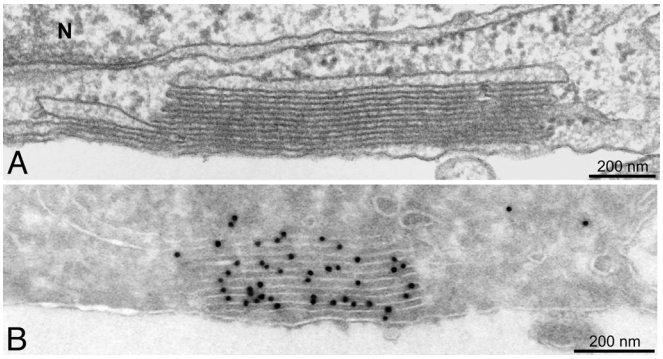

Fig. 4. A constitutively active mutant of STIM1 induces multilayered cortical ER elements. HeLa cells were transfected with a constitutively active STIM1 mutant. (*A*) These cells exhibited occasionally highly developed stacks of thin ER cisternae apposed to the PM. Of the entire stack, only one cisterna established a direct contact with the PM. (*N*) nucleus. (*B*) Labeling of cryosections with an anti-GFP antibody revealed the accumulation of mutant YFP-STIM1 in these stacks.

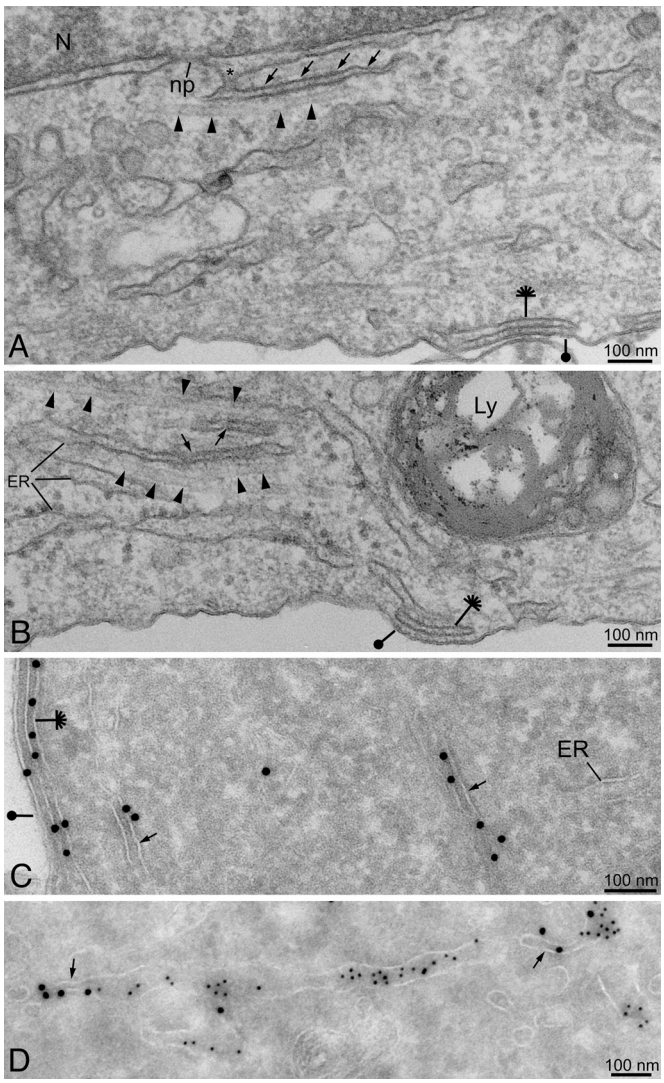

Fig. 5. Precortical ER can form in the cytosol. HeLa cells transfected with YFP-STIM1 and treated with Tg were fixed and processed for electron microscopy. (*A* and *B*) In Epon sections, thinner regions of the ER deprived of ribosomes (arrows) were seen aligned along microtubules (arrowheads). These elements were still connected to ER cisternae (ER) or to the nuclear envelope (star). Their morphology was similar to that of cER (asterisks) apposed to the PM (closed circles). Ly, lysosome; N, nucleus; np, nuclear pore. (*C*) In cryosections, labeling with an anti-GFP antibody (15-nm diameter gold) revealed a high concentration of YFP-STIM1 in cytosolic precortical elements. (*D*) In sections colabeled with an anti-BiP antibody (10-nm diameter gold) exclusion of BiP from thin YFP-STIM1-enriched domains was visible.

Discussion

In this study, detailed ultrastructural analysis revealed the existence of three distinct structures derived from conventional ER: precortical ER, cortical ER, and thin cortical ER.

Precortical ER elements were identified as thin ER subdomains, free of ribosomes, enriched in STIM1, depleted of BiP, and devoid of any contact with the PM. These structures may be equivalent to the STIM1-enriched domains observed previously by fluorescence microscopy, which were proposed to form as a result of interactions between STIM1 and EB1, a microtubule plus-end tracking protein (12). Indeed, a close relationship between precortical elements and microtubules was often apparent. It is likely that precortical ER represents an early step in the formation of functional cER. We speculate that upon ER calcium depletion, precortical elements are apposed to the PM, causing a large increase in the amount of cER in stimulated cells.

Cortical ER is formed by large sheets of ER closely apposed to the PM, but still physically connected to conventional ER cisternae. Remarkably, we observed within cER sheets a distinct subdomain, thinner, deprived of attached ribosomes, depleted of BiP, and enriched in STIM1. We speculate that thin cortical ER may correspond to regions where interactions between STIM1 luminal domains on opposite membranes bring together the two membranes and drive the exclusion of luminal proteins, such as BiP. Compared to cER regions exhibiting ribosomes, thin cER may represent a region specialized in calcium signaling and not engaged in protein synthesis and folding. Previous work has reported the occurrence of cortical ER devoid of attached ribosomes in a variety of cell types, most prominently neurons (13, 14), illustrating the ubiquitous nature of these structures in physiological situations.

STIM1-induced cER described in the present study most likely corresponds at least partially to previously described STIM1-enriched ER tubules identified in cells expressing HRP-STIM1 (6, 10). Indeed, the size of these structures, as well as the increase in their abundance upon Tg stimulation (+250%), were similar (10). On the other hand, the cER described here differs in several respects from earlier studies, notably concerning its detailed morphology and its proximity from the PM. We measured a distance between the PM and cER ranging from 3.8 to 16.9 nm (average, 11.3 nm) in cryosections, and from 1.3 to 14.7 nm (average 8.3 nm) in Epon sections. This was clearly different from previous observations in Epon sections, where the minimal distance observed between the PM and 200-nm segments of HRP-STIM1 tubules ranged from 10 to 25 nm (average, 17 nm) (10, 11). Our observations are compatible with long-range interactions between the PM and cER (>10 nm) as proposed previously (11), but in some regions of closer proximity short-distance interactions may take place. However, this interpretation is speculative, and the exact functional significance of these observations remains to be established.

The observation that BiP and GFP-KDEL are largely excluded from cER has important practical consequences. Notably, this would lead to underestimate the accumulation of ER at the cell periphery when it is identified with markers such as GFP-KDEL or HRP-KDEL. This may explain why we observed in this study, both in nontransfected and in YFP-STIM1-transfected cells, a much more prominent accumulation of ER at the cell periphery in Tg-treated cells (approximately + 300%) than seen in previous studies (+50%) (5, 10). However, the use of different cell lines may account for some of the differences between the present work and previous studies. In HeLa cells, our results suggest that the Tg-induced translocation of STIM1 to the cortical region is achieved by a marked increase in the amount of cER, rather than by an accumulation of STIM1 in preexisting structures. This conclusion is also in agreement with our observation that in transfected cells the concentration of YFP-STIM1 in cER did not change upon Tg stimulation.

Our knowledge of the mechanisms underlying the formation of functional cortical ER is progressing rapidly. New molecules involved are being identified at a fast pace. High-resolution electron microscopy will be essential to provide an integrated view of this complex process. Information about the occurrence and morphology of cER in various cell types exposed to physiological stimuli would also help to clarify the functional significance of this structure.

Methods

Cell Culture and Reagents. HeLa cells were grown in minimum essential medium containing 10% heat inactivated FCS, 2-mM L-glutamine, 100 units/ml penicillin, 100 μg/ml streptomycin at 37 °C, and 5% CO_2. For all experiments, cells were plated in 35-mm diameter cell-culture dishes and cotransfected with plasmids (2 μg) coding for the indicated proteins using Lipofectamine 2000. All experiments were performed 2 days after transfection.

Minimum essential medium, FCS, and Lipofectamine 2000 were purchased from Invitrogen. Thapsigargin was from Sigma. Plasmid for expression of YFP-STIM1 (Addgene plasmid 19756) was a generous gift from Anant Parekh (Oxford, U.K.). Site-directed mutations of YFP-STIM1 were generated using QuikChange (Stratagene) to generate the constitutively active mutant YFP-STIM1 D76A/D78A (4). The vector encoding GFP-KDEL was from Invitrogen (pCMV/myc/ER/GFP).

Electron Microscopy. For conventional electron microscopy, cells were fixed with 2% glutaraldehyde buffered with 0.1 M sodium phosphate, pH 7.4, en bloc stained with uranyl acetate (15), postfixed with osmium tetroxide, dehydrated in ethanol, and embedded in Epon. After sectioning, the samples were observed in a Tecnai Transmission electron microscope (FEI). For quantification of the amount of cortical ER, the AnalySIS software was used.

For immunoelectron microscopy, cells were fixed with 2% paraformaldehyde and 0.2% glutaraldehyde and processed for cryo-ultramicrotomy as described (16). Ultrathin frozen sections were prepared and incubated for immunolabeling as described (17).

The primary antibodies were affinity purified rabbit polyclonal anti-GFP (Abcam) and mouse monoclonal anti-Grp78/BiP antibody (StressGen Biotechnology). The anti-GFP antibody was diluted 1:200 and was labeled with goat anti-rabbit IgG gold (gold size, 15 nm). The anti-BiP antibody was used at 1:20 dilution and was labeled with goat anti-mouse IgG gold (gold size, 10 nm).

The evaluation of the labeling density of GFP and BiP was performed using the image analysis software Leica QWin Standard (Leica Imaging Systems Ltd.) and a Wacom graphic-pen tablet on electron micrographs at the final magnification ×93500. The density of the BiP (respectively GFP) labeling was expressed as the number of gold particles per square micrometer (respectively μm) of ER.

Fluorescence Microscopy. mCherry-STIM1 and ER-GFP fluorescence images from live cells grown on glass coverslips were acquired using a Plan-Apochromat 63x NA 1.4 oil-immersion objective on a confocal microscope (LSM510; Carl Zeiss AG). To compare fluorescence distribution of each fluorophore in the same voxels, the pinhole diameter was adjusted so that the axial resolution was the same on each channel (voxel size: 0.09 × 0.09 × 1 μm). Image processing was carried out using the Metamorph 7.5 software (Molecular Devices–Visitron Systems GmbH).

ACKNOWLEDGMENTS. We thank A. Widmer, M. T. E. Malek, and C. Castelbou for technical assistance, and N. Dupont and S. Arnaudeau for image processing. The Pôle Facultaire de Microscopie Ultrastructurale and the Bioimaging Core Facility at the University of Geneva Medical School provided access to electron microscopy and confocal microscopy equipment. This research was supported by grants from the Swiss National Science Foundation (to L.O., N.D., and P.C.).

1. Berridge MJ (2002) The endoplasmic reticulum: A multifunctional signaling organelle. *Cell Calcium* 32:235–249.
2. Lewis RS (2007) The molecular choreography of a store-operated calcium channel. *Nature* 446:284–287.
3. Stathopulos PB, Zheng L, Li GY, Plevin MJ, Ikura M (2008) Structural and mechanistic insights into STIM1-mediated initiation of store-operated calcium entry. *Cell* 135:110–122.
4. Liou J, et al. (2005) STIM is a Ca2+ sensor essential for Ca2+-store-depletion-triggered Ca2+ influx. *Curr Biol* 15:1235–1241.
5. Baba Y, et al. (2006) Coupling of STIM1 to store-operated Ca2+ entry through its constitutive and inducible movement in the endoplasmic reticulum. *Proc Natl Acad Sci USA* 103:16704–16709.
6. Luik RM, Wu MM, Buchanan J, Lewis RS (2006) The elementary unit of store-operated Ca2+ entry: Local activation of CRAC channels by STIM1 at ER-plasma membrane junctions. *J Cell Biol* 174:815–825.
7. Yuan JP, et al. (2009) SOAR and the polybasic STIM1 domains gate and regulate Orai channels. *Nat Cell Biol* 11:337–343.
8. Park CY, et al. (2009) STIM1 clusters and activates CRAC channels via direct binding of a cytosolic domain to Orai1 *Cell* 136:876–890.
9. Gwozdz T, Dutko-Gwozdz J, Zarayskiy V, Peter K, Bolotina VM (2008) How strict is the correlation between STIM1 and Orai1 expression, puncta formation, and ICRAC activation? *Am J Physiol Cell Physiol* 295:C1133–C1140.
10. Wu MM, Buchanan J, Luik RM, Lewis RS (2006) Ca2+ store depletion causes STIM1 to accumulate in ER regions closely associated with the plasma membrane. *J Cell Biol* 174:803–813.
11. Varnai P, Toth B, Toth DJ, Hunyady L, Balla T (2007) Visualization and manipulation of plasma membrane-endoplasmic reticulum contact sites indicates the presence of additional molecular components within the STIM1-Orai1 complex. *J Biol Chem* 282:29678–29690.
12. Grigoriev I, et al. (2008) STIM1 is a MT-plus-end-tracking protein involved in remodeling of the ER. *Curr Biol* 18:177–182.
13. Fiori MG, Mugnaini E (1981) Subsurface and cytoplasmic cisterns associated with mitochondria in pyramidal neurons of the rat dorsal cochlear nucleus. *Neuroscience* 6:461–467.
14. Rosenbluth J (1962) Subsurface cisterns and their relationship to the neuronal plasma membrane. *J Cell Biol* 13:405–421.
15. Tandler B (1990) Improved uranyl acetate staining for electron microscopy. *J Electron Microsc Tech* 16:81–82.
16. Volchuk A, et al. (2000) Megavesicles implicated in the rapid transport of intracisternal aggregates across the Golgi stack. *Cell* 102:335–348.
17. Liou W, Geuze HJ, Slot JW (1996) Improving structural integrity of cryosections for immunogold labeling. *Histochem Cell Biol* 106:41–58.